Nafie, L. A., Pezolet, M., & Peticolas, W. L. (1973) *Chem. Phys. Lett. 20*, 563–567.

Nagai, K., Hori, H., Morimoto, H., Hayashi, A., & Taketa, F. (1979) *Biochemistry 18*, 1304–1308.

Nagai, K., Kitagawa, T., & Morimoto, H. (1980) *J. Mol. Biol. 136*, 271–289.

Nozaki, Y., & Tanford, C. (1967) *Methods Enzymol. 11*, 733–746.

Perutz, M. F., Pulsinelli, P. D., & Ranney, H. M. (1972) *Nature (London), New Biol. 237*, 259–264.

Perutz, M. F., Kilmartin, J. V., Nagai, K., Szabo, A., & Simon, S. R. (1976) *Biochemistry 15*, 378–387.

Pulsinelli, D. D., Perutz, M. F., & Nagel, R. L. (1973) *Proc. Natl. Acad. Sci. U.S.A. 70*, 3870–3873.

Que, L., Jr., & Heistand, R. H., II (1979) *J. Am. Chem. Soc. 101*, 2219–2220.

Righetti, R., & Drysdale, J. W. (1971) *Biochim. Biophys. Acta 236*, 17–28.

Shelnutt, J. A., Rousseau, D. L., Friedman, J. M., & Simon, S. R. (1979) *Proc. Natl. Acad. Sci. U.S.A. 76*, 4409–4413.

Shibata, S., Miyaji, T., Iuchi, I., Ohba, Y., & Yamamoto, K. (1967) *Bull. Yamaguchi Med. Sch. 14*, 141–179.

Spaulding, L. D., Chang, C. C., Yu, N.-T., & Felton, R. H. (1975) *J. Am. Chem. Soc. 97*, 2517–2518.

Spiro, T. G. (1975) *Biochim. Biophys. Acta 416*, 169–187.

Spiro, T. G., & Strekas, T. C. (1974) *J. Am. Chem. Soc. 96*, 338–345.

Spiro, T. G., & Burke, M. J. (1976) *J. Am. Chem. Soc. 98*, 5482–5489.

Spiro, T. G., Stong, J. D., & Stein, P. (1979) *J. Am. Chem. Soc. 101*, 2648–2655.

Strekas, L. A., Packer, A. J., & Spiro, T. G. (1973) *J. Raman Spectrosc. 1*, 197–202.

Tatsuno, Y., Saeki, Y., Iwaki, M., Yagi, T., Nozaki, M., Kitagawa, T., & Otsuka, S. (1978) *J. Am. Chem. Soc. 100*, 4614–4615.

Teraoka, J., & Kitagawa, T. (1980) *J. Phys. Chem. 84*, 1928–1935.

Tomimatsu, Y., Kint, S., & Scherer, J. R. (1973) *Biochem. Biophys. Res. Commun. 54*, 1067–1074.

Tomimatsu, Y., Kint, S., & Scherer, J. R. (1976) *Biochemistry 15*, 4918–4924.

Tsubaki, M., Nagai, K., & Kitagawa, T. (1980) *Biochemistry 19*, 379–385.

Dynamics of an Interfacial Methylene in Dimyristoylphosphatidylcholine Vesicles Using Carbon-13 Spin Relaxation[†]

M. M. Fuson[‡] and J. H. Prestegard*

ABSTRACT: The dynamic and conformational properties of the 2-methylene on the *sn*-2 chain of dimyristoylphosphatidylcholine have been investigated in small unilamellar vesicles. An analysis of the spin relaxation of a proton-coupled ^{13}C nucleus has been used to provide the additional information necessary to propose a specific geometry for motion. The results suggest a model with three motions in addition to vesicle tumbling: (1) a slow axial rotation of the entire molecule about the bilayer normal ($\tau \simeq 2 \times 10^{-8}$ s); (2) torsional oscillations about C–C bonds on a very fast time scale; and (3) rapid jumps ($\tau = 6 \times 10^{-10}$ s) between two conformers having approximate gauche$^+$ and gauche$^-$ conformations about the C_2–C_3 bond of the *sn*-2 chain. The proposed conformations are compared to those previously predicted on the basis of crystal structures, spectroscopic data, and energy-minimization calculations.

The dynamic state of the lipid component of a biological membrane has been shown to affect a number of functional properties including transport (Chapman, 1975), immunochemistry (Parse et al., 1978), and enzyme activity (Moore et al., 1981). While it is often possible to establish correlations between dynamics and function in terms of rather poorly defined concepts, such as "fluidity", it is clear that an understanding of the precise way in which dynamics and function are linked in an anisotropic system such as a lipid bilayer will require more detailed pictures of motional properties.

Numerous spectroscopic techniques have now been applied to help define membrane motional properties (Grell, 1981). Among the more fruitful approaches has been a study of nuclear magnetic resonance (NMR) spin-relaxation times and line shapes (Chan et al., 1981; Jacobs & Oldfield, 1981; Seelig & Seelig, 1980). Several specific models for motion of lipid hydrocarbon chains have resulted (Pace & Chan, 1982; Gent & Prestegard, 1977; London & Avitable, 1977; Edholm, 1981). However, because of the limited number of parameters measured in conventional NMR studies, assignment of motional correlation times to specific chain motions is difficult and often based as much on physical intuition as experimental data. Recently, it has been shown that by studying the coupled spin relaxation of a ^{13}C-labeled lipid methylene group ($^{13}CH_2$), sufficient additional parameters can be measured to begin to assign correlation times to specific motions (Fuson & Prestegard, 1983). The recent work focused on a fatty acid dissolved in a lipid bilayer, and results are perhaps most relevant for lipid acyl chain motions in regions relatively unconstrained by lipid backbone geometry and interfacial effects.

The reason that ^1H-coupled ^{13}C spin-relaxation studies of a methylene group offer sensitivity to additional geometric and dynamic parameters is closely linked to an ability to separate autocorrelation and cross-correlation spectral densities. Most ^{13}C spin-relaxation studies of methylenes ignore the existence of cross-correlation spectral densities, assuming that dipolar

---

[†] From the Department of Chemistry, Yale University, New Haven, Connecticut 06511. *Received August 4, 1982.* This work was supported by a grant from the National Institutes of Health (GM 19035).

[‡] Present address: Department of Chemistry, University of Utah, Salt Lake City, UT 84112.

0006-2960/83/0422-1311$01.50/0

interactions between carbon and each directly bonded proton contribute independently to relaxation. While this assumption normally leads to only small errors in analysis, it discards potentially useful motional information (Hubbard, 1958; Kuhlman et al., 1970). The two dipolar interactions are always related by rotation about an axis perpendicular to the methylene plane. Separate measurement of cross-correlation spectral densities introduces sensitivity to reorientation of this rotation axis. Thus, a rotation vector in addition to the two ^{13}C–^{1}H dipolar vectors is available to define geometry of motion. There are a number of examples where inclusion of cross-correlation spectral densities has allowed complete determination of a diffusion tensor from spin relaxation of a single methylene group (Fuson & Prestegard, 1982; Mayne et al., 1976). For a fatty acid in a bilayer membrane, it has led to a model in which (1) the molecule as a whole is undergoing slow axial rotation, $\tau = 2 \times 10^{-7}$ s, (2) rapid jumps between trans and gauche conformations are taking place on a time scale of 4×10^{-11} s, (3) torsional jittering about bonds occurs on a picosecond time scale, and (4) isotropic rotation of the entire vesicle occurs on a time scale of 10^{-6} s. This model will be the starting point for analysis of data to be presented here.

In the present work we wish to extend coupled relaxation measurements to a phospholipid in a bilayer membrane and to focus on dynamics at the interfacial region. Specifically, we will look at the interface region through an examination of the dynamics of the 2-methylene of the *sn*-2 chain of dimyristoylphosphatidylcholine (DMPC).

Data will be presented in terms of line widths and magnetization modes, which are linear combinations of intensities for the outer lines and singlet and triplet components of the central line of the ^{1}H-coupled ^{13}C-labeled methylene multiplet. We use a slight modification of the nomenclature of Werbelow et al. (1978) in which ν_1 is the total ^{13}C intensity, ν_3 is the difference between outer-line and inner-line intensities, and ν_4 is the difference in the intensity of an outer line and the intensity of the triplet component of the inner line.

The spin system is prepared in various initial states: for example, ^{13}C inversion or ^{1}H inversion of the entire spin system. The time course of recovery of the modes is then monitored in analogy to the conventional T_1 inversion–recovery experiment. Only observation of ν_4 is done indirectly by application of a sampling pulse just before acquisition (Fuson & Prestegard, 1980).

The recovery is described by a series of linear differential equations that couple each of the modes. The coefficients in these equations are linear combinations of spectral densities that can be fit to recovery curves by a direct-search least-squares analysis. The spectral densities can be used to deduce motional parameters. Alternatively, correlation times for various motional models can be fit directly. The analysis as applied to fatty acid data has been given elsewhere (Fuson & Prestegard 1983) and will not be repeated in detail here.

One new element, however, must be pointed out. In preceding work, we have assumed that the protons of the methylene group are equivalent; this is not entirely correct here. For phosphatidylcholines in solution the C_2 protons on the *sn*-2 chain have distinct chemical shifts, and the motions they execute in anisotropic environments will be different. Since the chemical shift differences are small compared to proton line widths in vesicles, it should be acceptable to continue to treat relaxation with the formalism developed for an AX_2 spin system. Motional inequivalence will, however, be recognized in that the spectral densities J_{CH1CH1} and J_{CH2CH2}, which are the autocorrelation spectral densities describing the motion of the dipolar vectors C–H1 and C–H2, respectively, will no longer be identical. This applies to the cross-correlation densities such as $J_{CH1H1H2}$ and $J_{CH2H2H1}$ as well, and the number of dipolar spectral densities occurring in the analysis is expanded from 13 to 19.

Experimental Procedures

Isotopically labeled materials were obtained as follows: [2-^{13}C]acetic acid (90 atom % ^{13}C), $^{2}H_2SO_4$ (96 atom % ^{2}H), and $LiAl^{2}H_4$ (99 atom % ^{2}H) were from MSD Isotopes, Merck and Co. (Rahway, NJ). $^{2}H_2O$ (99.75 atom % ^{2}H) was from J. T. Baker Chemical Co. (Phillipsburg, NJ). L-α-Lysophosphatidylcholine (γ-myristoyl) was obtained from Calbiochem (LaJolla, CA). All other chemicals were reagent grade and obtained from local suppliers.

Synthesis of 2-[2-^{13}C]-DMPC. [2-^{13}C,3,3,4,4-$^{2}H_4$]Myristic acid was synthesized as previously described (Fuson & Prestegard, 1983). 2-[2-^{13}C]-DMPC was synthesized by acylating lyso-DMPC according to the general procedure of Mason et al. (1981). So that labeled material could be conserved, however, the anhydride was generated in situ by using the following modifications. Lysophosphatidylcholine (0.5 mM) is suspended in dry $CHCl_3$. To this is added 1 mol equiv of labeled fatty acid, 3 mol equiv of dicyclohexylcarbodiimide, and 1 mol equiv of 4-pyrrolopyridine as catalyst for the acylation. This mixture is stirred at room temperature for several days and then labeled DMPC separated as described by Mason et al. (1981). Elution from the final silicic acid column yielded a fraction of phosphatidylcholine migrating as a single spot on TLC[1] and a fraction of nearly equal mass contaminated by appreciable amounts of lysophosphatidylcholine. The pure fraction used in subsequent experiments represented 23% of theoretical yield.

NMR Sample Preparation. A total of 80 mg of 2-[2-^{13}C]-DMPC was suspended in 1.3 mL of $^{2}H_2O$ buffer (0.1 M PO_4^{2-}, 0.02% NaN_3, 0.5 mM EDTA) by vortexing and the $p^{2}H$ adjusted to 7.4 with $NaO^{2}H$. Small unilamellar vesicles were made by sonicating this suspension for 6 h at 50 °C in a Branson Model E bath sonicator. The resulting vesicle solutions were placed in 10-mm NMR tubes and stored at temperatures above 30 °C. The multilayer sample was prepared analogously except that instead of being sonicated, the sample was heated to 50 °C for 6 h with frequent vortexing. Samples were not degassed as previous work had shown full NOEs to be present without this precaution.

NMR Experiments. All spectra were acquired at 40 ± 1 °C on a Bruker CXP-200 spectrometer. NMR relaxation experiments are analogous to standard 180°–τ–90° inversion–recovery experiments and were performed as outlined previously (Fuson & Prestegard, 1982, 1983). A total of 800 scans was accumulated for each of 12 τ values ranging in time from 2 ms to 3 s with an additional recycle delay of 3 s. Each spectrum covered a width of 4000 Hz and was collected in 4K data points. Intensity values were obtained for the low-field and central peaks of the 2-^{13}C multiplet directly from peak amplitudes. A factor to adjust for differences in line widths was obtained by requiring $\nu_3(\infty)$ to be zero.

Results

The results of a ^{13}C inversion–recovery experiment on 2-[2-^{13}C]-DMPC sonicated vesicles are shown in Figure 1. The

---

[1] Abbreviations: TLC, thin-layer chromatography; EDTA, ethylenediaminetetraacetic acid; CSA, chemical shift anisotropy.

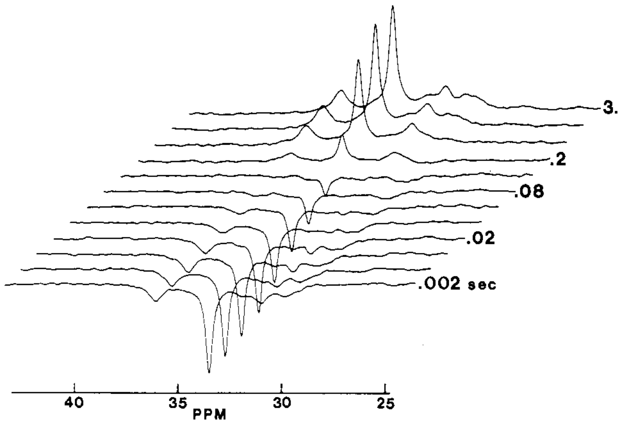

FIGURE 1: ^{13}C inversion–recovery sequence for 2-[2-^{13}C]-DMPC sonicated vesicles. The pulse sequence is 180°(^{13}C)–τ–90°(^{13}C)–AQ.

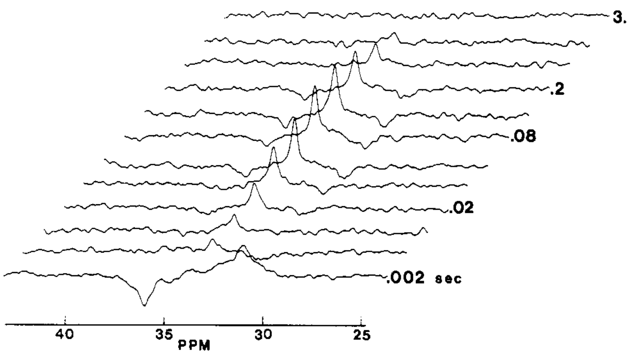

FIGURE 2: ^{13}C difference spectra showing evolution of ν_4 after ^{1}H inversion for 2-[2-^{13}C]-DMPC sonicated vesicles. Spectra shown are the difference between data acquired with a 180°(^{1}H)–τ–90°(^{1}H,^{13}C)–AQ and with a 180°(^{1}H)–τ–90°(^{13}C)–AQ pulse sequence.

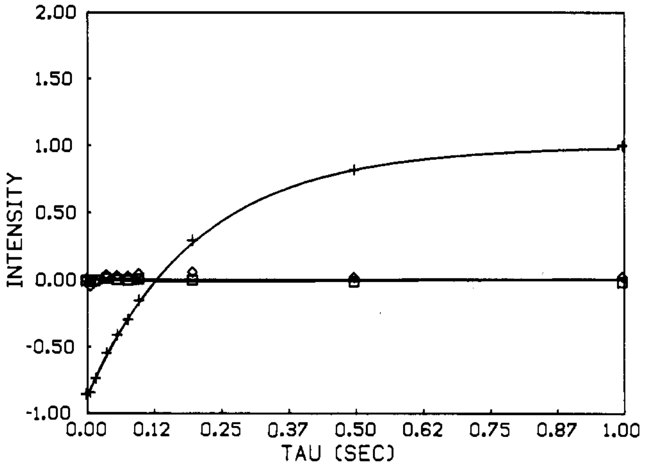

FIGURE 3: Time evolution of magnetization modes after ^{13}C inversion. Modes are defined in the text. Intensities are normalized so that the equilibrium ^{13}C intensity is 1. (+) ν_1; (◇) ν_3; (□) ν_4. Solid lines are calculated from the isotropic plus axial fit (column 2 of Table I).

main feature is the multiplet arising from the isotopically enriched C2 methylene of the *sn*-2 chain, but the upfield peak is partially obscured by the background resonances from natural abundance ^{13}C in other lipid methylenes. Careful examination of the spectra obtained near the null points shows that the outer lines are relaxing slightly faster than the inner line. Similar spectra following the time evolution of ^{13}C after inversion of ^{1}H were obtained. The main time-dependent feature here is the growth and subsequent decay of the ^{13}C magnetization after the ^{1}H pulse.

The downfield and central resonances of the enriched multiplet are sufficiently well resolved that their intensities may be measured directly, without having to resort to difference spectra as we did with the fatty acid study. The outer line, corresponding to a single transition, will be a single Lorentzian. We can measure its intensity directly from its amplitude. The shape of the inner line can be more complex. However, in the limit where isotropic motions are slow compared to the Larmor precession frequency (ω_0) but rapid compared to the magnitude of the dipolar coupling, it reduces to a single Lorentzian (Prestegard & Grant, 1978). In the fatty acid case the only isotropic motion needed to fit the data was vesicle tumbling. On the basis of radii measured in the light scattering experiments described in that study and adjusting for changes in temperature, we can calculate that $\tau_c = 2 \times 10^{-6}$ s for the analogous motion in this system (Fuson & Prestegard, 1983). Compared to $1/\omega_0 = 3 \times 10^{-9}$ s, this is certainly in the slow limit. It is also rapid in comparison to the reciprocal of the dipolar splittings. Further confirmation of the validity of the assumption is provided by the free fatty acid study where we were able to predict the central-line width, on the basis of specific motional models, the slow motion assumption, and parameters measured from spin–lattice relaxation data. We shall therefore also take central-line intensities directly from the amplitudes.

The spectra shown are sufficient to measure the magnetization modes ν_1, the total ^{13}C magnetization of the ^{13}CH$_2$ spin system, and ν_3, the difference between the sum of the outer-line intensities and the inner-line intensity. To measure ν_4, the difference between the outer-line intensity and the inner-line triplet component intensity, we must perform a second set of experiments utilizing a ^{1}H intensity-exchange pulse and take difference spectra using the two sets of experiments (Fuson & Prestegard, 1980, 1982, 1983). The results of such a procedure after initial ^{1}H inversion are shown in Figure 2. The magnetization is observed to grow into the central line and then decay away to the ν_4 equilibrium value of zero. The anomalous appearance of the $\tau = 2$ ms spectrum is very likely due to the excitation of double-quantum coherence: intensity is transferred from the downfield resonance (^{1}H state $\alpha\alpha$) to the upfield resonance (^{1}H state $\beta\beta$). We see this here because of the imperfect nature of our 180° pulses (^{1}H pulses are applied through the low-power decoupler circuitry of the spectrometer and no phase cycling was available) and because at $\tau = 2$ ms the magnetization is not yet randomized in the *XY* plane.

The time courses of ν_1, ν_3, and ν_4 after ^{13}C inversion are shown in Figure 3. Qualitatively, the data appear very similar to that obtained for our earlier study of the fatty acid dynamics except that the magnitudes of ν_3 and ν_4 are even smaller. The time courses of ν_1, ν_3, and ν_4 after ^{1}H inversion are shown in Figure 4. Following proton inversion, all modes reach significant amplitudes, reflecting the greater magnitude of the proton magnetization. In comparison to the fatty acid data, ν_4 after ^{1}H inversion only reaches half the amplitude observed in the earlier study.

In addition to the time courses of the longitudinal modes described above, we shall use the multiplet line widths as a point of comparison for our dynamic modeling. We measure the outer-line widths as 33 Hz ($R_2 = 103$ s^{-1}) and the inner-line width as 11 Hz ($R_2 = 35$ s^{-1}). Compared to the fatty acid case (60 and 8 Hz), this shows a narrowing of the outer lines and a slight broadening of the inner line.

It now remains to fit the above data to specific motional models. The fatty acid work showed that a model based on

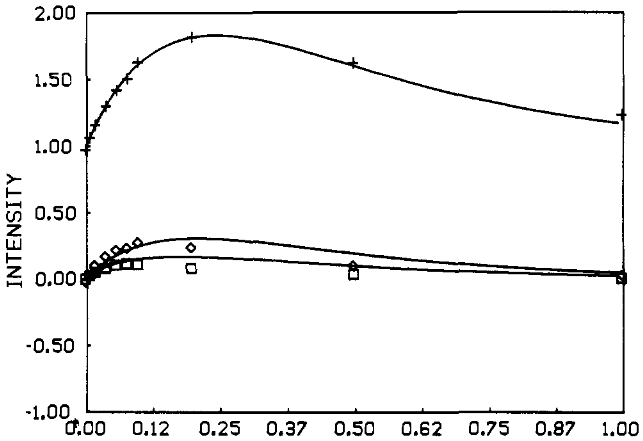

FIGURE 4: Time evolution of magnetization modes after ^1H inversion. Modes are defined in the text. Intensities are normalized so that the equilibrium ^{13}C intensity is 1. (+) ν_1; (◇) ν_3; (□) ν_4. Solid lines are calculated from the isotropic plus axial fit (column 2 of Table I).

Table I: Fits to Dynamic Models[a]

model	isotropic + axial	iso + axial + 3 site	iso + axial + 2 site	iso + axial + 2 site + torsion
τ_i	$(5.8 \pm 0.3) \times 10^{-8}$	$[2 \times 10^{-6}]^c$	$[2 \times 10^{-6}]^c$	$[2 \times 10^{-6}]^c$
τ_1	$(2.1 \pm 0.2) \times 10^{-11}$	$(5.5 \pm 0.6) \times 10^{-9}$	$(6.3 \pm 0.5) \times 10^{-9}$	$(1.9 \pm 0.2) \times 10^{-8}$
τ_2		$(1.2 \pm 0.1) \times 10^{-10}$	$(1.5 \pm 0.1) \times 10^{-10}$	$(6.2 \pm 0.5) \times 10^{-10}$
θ_{CH_1}	=60°			
θ_{CH_2}	=85°			
S				0.56 ± 0.01
P_{g^+}		50	51	53
P_{g^-}		47	49	47
P_t		3		
$\chi^{2\,b}$	1.22	6.71	6.80	2.41

[a] All units are in seconds. [b] χ^2 of fit to longitidinal modes only. [c] This parameter held constant in the fit.

simple axial diffusion could, under some circumstances, produce resonable fits to the data. Thus, we first allow only slow isotropic motions and a fast axial rotation, allowing the orientation of the methylene relative to the axis of rotation to vary. By doing this, in the fatty acid study we were able to show that the dominant rapid axial motion was not about the bilayer normal but could be better modeled by rotation about a C–C bond axis. The results of such a model as applied to labeled phospholipid are summarized in column 2 of Table I. The data are fit by allowing the two C–H vectors to assume angles of 60 and 85° with respect to the rotation axis. χ^2 is given as a measure of goodness of fit and in this case is among the best values we can achieve. Theoretical recovery curves generated are shown in Figures 3 and 4.

The best fit angles can be compared to a model that allows rotation about a C–C bond. In this model, the C–H vectors are at an angle of 70.5°. Another simple model is to assume that the lipids are in their crystallographic conformation (Pearson & Pascher, 1979) and that the rotation is about the bilayer normal. Then the C–H vectors are at angles of approximately 30 and 90° to the rotation axis. Although the model fits the data well, no simple conformational interpretation is possible.

Another commonly employed and intuitively appealing model allows jumps between discrete conformers. For our initial jump model we shall assume that the 2-carbon of the *sn*-2 chain can assume three conformations: perfect trans (t), gauche$^+$ (g$^+$), and gauche$^-$ (g$^-$) isomers generated by rotations about the C_2–C_3 bond above an otherwise all-trans acyl chain extending normal to the bilayer surface. As our "rest state", we begin with the g$^-$ isomer, which is very similar to the conformation observed in crystal structures of various phospholipids (Hauser et al., 1981). From this state we assume jumps can take place to either t or g$^+$ conformers. We shall allow the populations of the conformers to be parameters of the model. Relative jump rates are fixed by populations and by assuming that the jump rates to g$^-$ are the same from both conformers. The latter is an arbitrary assumption, but as we shall see, alteration of relative rates does not improve our fit. In fact, gauche to trans jumps are not necessary.

The results of fitting the above model, which also includes vesicle tumbling and a freely fit axial diffusion about the bilayer normal, are shown in Table I, column 3. In addition to conformer populations, P_i, parameters listed are τ_i, the isotropic tumbling time, τ_1, the correlation time for axial diffusion, and τ_2, the reciprocal of the gauche to trans jump rate. Although hardly optimum, the fit is good for such a simple and intuitively appealing model. Even line widths are reproduced well. The outstanding characteristic of the fitted model is the nearly equal distribution of population between g$^-$ and g$^+$ states with virtually no t state. This suggests that a two-site jump model may describe the dynamics quite well. Indeed, as shown in column 4 of Table I, a two-site model involving only g$^-$ and g$^+$ gives a virtually identical fit.

Our work with the free fatty acid system showed that introduction of a wobble about the director axis in order to model torsional bond oscillations on a picosecond time scale fit the data best. If we apply an analogous model here, which includes the two-site jump just discussed, the results shown in column 5 of Table I are obtained. Further significant improvements in the fit do occur. χ^2 approaches that found for the axial diffusion model.

Discussion

Models derived from spin relaxation data can never be presented with absolute certainty. This is particularly true where geometry is involved. Specific models can be stated to be consistent with observation but they are seldom unique solutions. In view of this, it is essential that we compare proposals with supplementary data relating to lipid structure and dynamics. In doing this, we will focus on the jump model, which is intuitively more appealing and where relationships to static structures are better defined.

Aside from vesicle tumbling, there are three motions to consider in the jump model: (1) a slow axial diffusion about the bilayer normal on a time scale of 1.9×10^{-8} s; (2) torsional oscillations about C–C bonds on a picosecond time scale; (3) a rapid jumping ($\tau = 6.2 \times 10^{-10}$ s) between rotational isomers, g$^+$, g$^-$, and t.

The axial diffusion very likely represents diffusion of the entire DMPC molecule in the bilayer. It is possible to predict the rate of diffusion on the basis of the Stokes–Einstein equation and modeling the lipid molecule as a cylinder. Using the measured surface area per DMPC (70 Å^2) (Reiss-Husson, 1967) and the bilayer half-thickness (21 Å) and choosing 50 cP as our value of the bilayer microviscosity [measured values range from 1 to 100 cP (Seelig & Seelig, 1980)], we calculate a correlation time of 1.7×10^{-8} s. The agreement is somewhat fortuitous given the crudity of our estimates of the parameters but nevertheless provides support for the model. It is important to note, however, that in our calculations we have used the acyl chain rather than the glycerol backbone as a reference. If we shift to the glycerol backbone as a frame of reference, the jumps between isomers will introduce an additional, but restricted, rotation about the diffusion axis at a more rapid time scale.

The torsional oscillations about C–C bonds on a picosecond time scale were introduced to alleviate many of the problems associated with overly restrictive jump models. We have modeled these motions by allowing the director axis to move in a cone of constant probability. This is intended to mimic the cumulative motion resulting from several C–C bond oscillations. In the data fitting, the degree of motion is characterized by an adjustable order parameter, S, which we find to be 0.56. If this movement is in a cone of constant probability, the value of S corresponds to a semiangle of 47°. It is identical with that observed in the fatty acid case and is not unreasonable in view of estimates of 20–30° oscillations for individual C–C bonds (Levy et al., 1979).

Jumps between discrete conformers are characterized by both time scale and geometry. The time scale observed is consistent with the fast time scale measured in lipid systems in numerous studies (Chan et al., 1981; Brown et al., 1979; London & Avitabile, 1977; Lee et al., 1976; Van der Leeuw & Stulen, 1981). Bond isomerizations in simple hydrocarbons at ambient temperature are also believed to be on the order of 10^{-10} s (Levy et al., 1979). Thus, the time scale is reasonable.

More unexpected is the apparent two-sited nature of the conformational jumps with g^+ and g^- conformers represented equally. Crystal structures of dilauroylphosphatidylethanolamineacetic acid (Hitchcock et al., 1974) and DMPC dihydrate have been obtained (Pearson & Pascher, 1979; Hauser et al., 1981). The structures show distinct similarities about the glycerol backbone and *sn*-2 chain. The observed conformation is characterized by alignment of the glycerol backbone more or less parallel to the bilayer normal with the *sn*-1 chain extending directly down into the bilayer. The *sn*-2 acyl chain, on the other hand, starts out perpendicular to the bilayer normal and turns down at the 2-carbon. In the region of the C_2 methylene, bond angles about the O–C, C_1–C_2, and C_2–C_3 bonds are in the ranges 172–179°, 279–226°, and 45–67°, respectively. From the point of view of the all-trans terminal portion of the acyl chain, this is a g^- conformation at the C_2–C_3 bond. The general characteristics of the glycerol backbone conformation are believed to be retained in aqueous dispersions of bilayers as well. This is supported by a variety of experimental data (Zaccai et al., 1979; Seelig & Seelig, 1974; Vaz et al., 1979; Wittebort et al., 1981). Thus, postulation of existence of at least the g^- isomer in the liquid-crystalline bilayer phase seems reasonable.

There is no direct evidence for the g^+ isomer. However, an examination of the literature shows that two backbone conformers of nearly equal probability were predicted by MacAlister et al. in 1973 using energy-minimization calculations. These conformations are shown in Figure 5.

Conformation A is characterized by a g^- conformation at the C_2–C_3 bond of the *sn*-2 chain as is observed in the recent crystal structures. This conformation differs from the crystal structures, however, in that the glycerol C_1–C_2–C_3–O angle (θ_3 in MacAlister's notation) is 60° as opposed to 180°, and a second angle, β_1, is at 150° as opposed to 90°. However, recent evidence from ^{2}H NMR of DMPC and dipalmitoylphosphatidylethanolamine (DPPE) gel-state multilayers labeled at the C_2 position of glycerol suggests that in these systems θ_3 exists in or near a gauche conformation (±60°) (Blume et al., 1982).

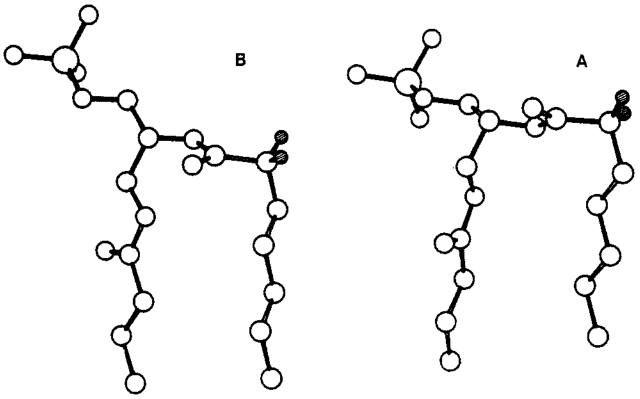

FIGURE 5: Proposed conformations for glycerol phosphate backbone in DMPC vesicles. Structures are those proposed by MacAlister et al. (1973). The protons on the C_2 methylene of the *sn*-2 chain are depicted as cross-hatched atoms.

Conformation B has the conformation observed in crystal structures at θ_3 but predicts a g^+ conformation at the *sn*-2 C_2–C_3 bond. A jump from conformation A to B or a jump from B to the crystal-structure conformation would be expected to approximate the motion that fits our data.

The proposed g^- to g^+ jumps can be compared to motional models previously proposed for conformations in multilayer systems. The ^{2}H NMR data of Seelig have led to one model involving three chain conformers. On the basis of the statistical theories of Marcelja (1974), Seelig interprets the ^{2}H results as being caused by finite probabilities of the initial segment of the chains being in trans and g^+ conformations as well as the crystallographic conformation in which the initial segment is perpendicular to the bilayer normal (Schindler & Seelig, 1975).

Solid-state ^{13}C NMR studies of the ester carbonyl of the *sn*-2 chain in liquid-crystaline phosphatidylcholine multilayers have also led to proposed motional models. Cornell (1980), on the basis of calculated CSAs for conformers suggested by the theoretical work of Gupta et al. (1975), suggests that the small 5–7-ppm CSA of the *sn*-2 carbonyl is characteristic of rapid jumps between conformers that are gauche and trans at the C_2–C_3 bond. The trans conformation is explicitly excluded by our fitting procedure, and we must conclude that either the gauche–trans model is not a unique fit to the multilayer data or lipids in vesicle and multilayer forms differ in motional character. With respect to the ^{13}C data, our results are more in accord with the interpretation of Wittebort et al. (1981) in which shielding is small due to the unique angle of the carbonyl relative to the bilayer normal. The orientation of the C=O bond near the magic angle is possible under our model. The jumps we propose need have little effect on the absolute value of the C=O angle as seen in Figure 6 (−60 to +80).

As a more direct comparison of vesicle and multilayer systems, we have measured the width of the inner line of the ^{13}C multiplet of 2-[2-^{13}C]-DMPC in multilayers. The observed line width is 240 Hz. To simulate this line width, in addition to the axial rotation, conformational jumps, and torsions derived from the vesicle data, we must account for the effects of lateral diffusion in the multilayers. Lateral-diffusion constants have been measured for a number of phosphatidylcholines, and the values are generally in the range of (5–10) × 10^{-8} cm^2 s^{-1} (Sheets & McConnell, 1978; Kuo & Wade, 1979; Fahey & Webb, 1978). If we assume this value, assume an average radius of curvature of 1000 Å (Papahadjopoulos & Miller, 1967), and employ other motional parameters of our models, the predicted line width is in good agreement with our observation. In contrast, no matter what the effect of translational diffusion on rotational averaging in multilayers, a model including jumps among trans and gauche isomers will result in an almost infinitely sharp central methylene resonance.

The ability of the g^+–g^- jump model to predict deuterium order parameters measured on multilayer systems is not nearly so successful. However, we believe this to be the result of the choice of rather idealized bond geometries. The axial rotation model with less idealized CH angles relative to a rotation axis of 60 and 85°, for example, produces almost perfect agreement.

Thus, while the model may not be unique or perfect, we believe the g^+–g^- jump model provides a reasonable description of lipid motions in vesicle bilayer membranes. It also seems reasonable for more extended bilayer membranes. The conformational flexibility that exists at the membrane interface should have implications for surface recognition and transport.

Acknowledgments

We thank Virginia Miner for producing ORTEP diagrams of phospholipid conformers.

Registry No. L-Dimyristoylphosphatidylcholine, 18194-24-6.

References

Blume, A., Rice, D. M., Wittebort, R. J., & Griffin, R. G. (1982) *Biochemistry 21*, 6220–6230.

Brown, M. F., Seelig, J., & Haeberlen, U. (1979) *J. Chem. Phys. 70*, 5045–5053.

Chan, S. I., Bocian, D. F., & Petersen, N. (1981) in *Membrane Spectroscopy* (Grell, E., Ed.) p 150, Springer-Verlag, New York.

Chapman, D. (1975) *Q. Rev. Biophys. 8*, 185–235.

Cornell, B. A. (1980) *Chem. Phys. Lett. 72*, 462–465.

Edholm, O. (1981) *Chem. Phys. Lipids 29*, 213–224.

Fahey, P. F., & Webb, W. W. (1978) *Biochemistry 17*, 3046–3053.

Fuson, M. M., & Prestegard, J. H. (1980) *J. Magn. Reson. 41*, 179–184.

Fuson, M. M., & Prestegard, J. H. (1982) *J. Chem. Phys. 76*, 1539–1549.

Fuson, M. M., & Prestegard, J. H. (1983) *J. Am. Chem. Soc.* (in press).

Gent, M. P. N., & Prestegard, J. H. (1977) *J. Magn. Reson. 25*, 243–262.

Grell, E. (1981) in *Membrane Spectroscopy*, Springer-Verlag, New York.

Gupta, S. P., Govil, G., & Mishra, R. K. (1975) *J. Theor. Biol. 51*, 13–34.

Hauser, H., Pascher, I., Pearson, R. H., & Sundell, S. (1981) *Biochim. Biophys. Acta 650*, 21–51.

Hitchcock, P. B., Mason, R., Thomas, K. M., & Shipley, G. G. (1974) *Proc. Natl. Acad. Sci. U.S.A. 71*, 3036–3040.

Hubbard, P. S. (1958) *Phys. Rev. 109*, 1153–1158.

Jacobs, R. E., & Oldfield, E. (1981) *Prog. Nucl. Magn. Reson. Spectrosc. 14*, 113–136.

Kuhlman, K. F., Grant, D. M., & Harris, R. K. (1970) *J. Chem. Phys. 52*, 3439–3448.

Kuo, A., & Wade, G. B. (1979) *Biochemistry 18*, 2300–2308.

Lee, A. G., Birdsall, N. J. M., Metcalfe, J. C., Warren, G. B., & Roberts, G. C. K. (1976) *Proc. R. Soc. London, Ser. B 193*, 253–274.

Levy, R. M., Karplus, M., & McCammon, J. A. (1979) *Chem. Phys. Lett. 65*, 4–11.

London, R. E., & Avitable, J. (1977) *J. Am. Chem. Soc. 99*, 7765–7776.

MacAlister, J., Yathindra, N., & Sundaralingam, M. (1973) *Biochemistry 12*, 1189–1195.

Marcelja, S. (1974) *Biochim. Biophys. Acta 367*, 165–176.

Mason, J. T., Broccoli, A. V., & Huang, C.-H. (1981) *Anal. Biochem. 113*, 96–101.

Mayne, C. L., Grant, D. M., & Alderman, D. M. (1976) *J. Chem. Phys. 65*, 1684–1695.

Moore, B. M., Lentz, B. R., Hoechli, M., & Meissner, G. (1981) *Biochemistry 20*, 6810–6817.

Pace, R. J., & Chan, S. I. (1982) *J. Chem. Phys. 76*, 4217–4227.

Papahadjopoulos, D., & Miller, N. (1967) *Biochim. Biophys. Acta 135*, 624–638.

Parse, J. W., Henry, N., & McConnell, H. M. (1978) *Proc. Natl. Acad. Sci. U.S.A. 75*, 1515–1518.

Pearson, R. H., & Pascher, I. (1979) *Nature (London) 281*, 499–501.

Prestegard, J. H., & Grant, D. M. (1978) *J. Am. Chem. Soc. 100*, 4664–4668.

Reiss-Husson, F. (1967) *J. Mol. Biol. 25*, 363–382.

Schindler, H., & Seelig, J. (1975) *Biochemistry 14*, 2283–2287.

Seelig, A., & Seelig, J. (1974) *Biochemistry 13*, 4839–4845.

Seelig, J., & Seelig, A. (1980) *Q. Rev. Biophys. 13*, 19–61.

Sheets, J. R., & McConnell, H. M. (1978) *Proc. Natl. Acad. Sci. U.S.A. 75*, 4661–4663.

Van der Leeuw, Y. C. W., & Stulen, G. (1981) *J. Magn. Reson. 42*, 434–445.

Vaz, M. J., Vaz, N. A. P., Doane, J. W., & Westerman, P. W. (1979) *Biophys. J. 28*, 327–338.

Werbelow, L. G., Grant, D. M., Black, E. P., & Courtieu, J. M. (1978) *J. Chem. Phys. 69*, 2407–2419.

Wittebort, R. J., Schmidt, C. F., & Griffin, R. G. (1981) *Biochemistry 20*, 4223–4228.

Zaccai, G., Buldt, G., Seelig, A., & Seelig, J. (1979) *J. Mol. Biol. 134*, 693–706.